Dimensionless scaling of the critical beta for onset of a neoclassical tearing mode

R. J. La Haye, R. J. Buttery, S. Guenter, G. T. A. Huysmans, M. Maraschek et al.

Citation: Phys. Plasmas **7**, 3349 (2000); doi: 10.1063/1.874199
View online: http://dx.doi.org/10.1063/1.874199
View Table of Contents: http://pop.aip.org/resource/1/PHPAEN/v7/i8
Published by the American Institute of Physics.

Dimensionless scaling of the critical beta for onset of a neoclassical tearing mode

R. J. La Haye
General Atomics, P.O. Box 85608, San Diego, California 92186-5608

R. J. Buttery
Euratom/UKAEA Fusion Association, Culham Science Centre, Abingdon, OX14 3DB, United Kingdom

S. Guenter
Max-Planck Institut für Plasmaphysik, Garching, Germany

G. T. A. Huysmans[a)]
JET Joint Undertaking, Abingdon, United Kingdom

M. Maraschek
Max-Planck Institut für Plasmaphysik, Garching, Germany

H. R. Wilson
Euratom/UKAEA Fusion Association, Culham Science Centre, Abingdon, OX14 3DB, United Kingdom

(Received 3 March 2000; accepted 4 May 2000)

The islands from tearing modes driven unstable and sustained by the helically perturbed neoclassical bootstrap current often provide the practical limit to long-pulse, high confinement tokamak operation. The destabilization of such ''metastable'' plasmas depends on a ''seed'' island exceeding a threshold. A database from similar regimes [high confinement H-mode with periodic edge localized modes (ELMs) and periodic central sawteeth] was compiled from the tokamaks ASDEX Upgrade (AUG) [Plasma Phys. Controlled Fusion **41**, 767 (1999)], DIII-D [Nucl. Fusion **38**, 987 (1998)], and JET (Joint European Torus) [Plasma Phys. Controlled Fusion **41**, B1 (1999)]. A comparison is made of the measured critical beta for onset of the $m/n=3/2$ mode (m and n being the poloidal and toroidal Fourier harmonics, respectively) to a model in terms of dimensionless parameters for the seed and threshold islands. This modeling is then used for extrapolation to a reactor-grade tokamak design such as ITER/FDR (International Thermonuclear Experimental Reactor/Final Design Report) [Nucl. Fusion **39**, 2137 (1999)]; this indicates that the seed island from sawteeth could be too small to sufficiently disturb the metastable plasma and excite the $m/n=3/2$ neoclassical tearing mode. © *2000 American Institute of Physics.* [S1070-664X(00)02408-3]

I. INTRODUCTION

For a classical tearing mode, Δ' characterizes the free energy available in the current profile and must be positive to drive the instability.[1] However, even if $\Delta'<0$, a tearing mode can be destabilized and sustained by perturbing the neoclassical bootstrap current.[2] The $m/n=3/2$ islands of full radial width w, typically (but not always) excited by sawteeth, often constitute the first practical limit to low collisionality, high-beta, high-confinement, long-pulse tokamak operation in the existing tokamaks, Axisymmetric Divertor Experiment-Upgrade (ASDEX Upgrade),[3] DIII-D,[4] and Joint European Torus (JET)[5] when operated in a regime similar to that of the proposed reactor-grade tokamak International Thermonuclear Experimental Reactor/Final Design Report (ITER/FDR).[6] Data for the onset of these modes were obtained by slowly raising beta (ratio of volume averaged plasma pressure to that of the toroidal magnetic field) on a time scale longer than the sawtooth period and observing the beta value at onset. In this paper, a comparison of the measured critical beta to a theoretical model for the critical beta is made in terms of dimensionless parameters, and a semiempirical scaling law based on this model is developed. This modeling is then used for extrapolation to a reactor-grade tokamak, ITER/FDR in particular.

In Sec. II, the physics model for the neoclassical tearing mode onset is developed. Section III describes the experimental regime and database. The fitting of the model for the critical beta with dimensionless parameters is presented in Sec. IV with extrapolation to ITER/FDR. Conclusions are given in Sec. V.

II. PHYSICS MODEL FOR NTM CRITICAL BETA

A. Modified Rutherford equation

The growth (or decay) of tearing mode islands is given by the Rutherford equation modified for the perturbed neoclassical bootstrap current,[7]

$$\frac{\tau_R}{r^2}\frac{dw}{dt}=\Delta'+\epsilon^{1/2}(L_q/L_p)\beta_\theta\left[\frac{w}{w^2+w_d^2}-\frac{w_{\mathrm{pol}}^2}{w^3}\right]. \tag{1}$$

[a)]Present address: CEA Cadarache, France.

A helical magnetic perturbation resonant at minor radius r, where the equilibrium safety factor $q=m/n$, with m the poloidal mode number and n the toroidal mode number, generates a ''seed'' island of full width w which tends to flatten the pressure in the O-point of the island but not in the X-point. This makes a helical perturbation of the plasma pressure, resulting in a helical perturbation of the bootstrap current $J_{\|bs}\approx\epsilon^{1/2}\nabla p/B_\theta$, which can reinforce the original magnetic perturbation. This effect is destabilizing for the conventional case of a monotonically increasing q-profile with $L_q\equiv q/(dq/dr)>0$ and monotonically decreasing p-profile with $L_p\equiv -p/(dp/dr)>0$. Here Δ' is assumed negative, i.e., stabilizing, $\tau_R=\mu_0 r^2/(1.22\,\eta)$ is the resistive diffusion time for local plasma resistivity η, $\epsilon=r/R_0$ is the local inverse aspect ratio for major radius R_0, and β_θ is the poloidal beta, i.e., the plasma pressure relative to poloidal magnetic field pressure.

B. Characteristic island widths w_d and w_{pol} associated with moderating effects

Two effects moderate or limit the perturbed bootstrap current term of Eq. (1). The term w_d is a characteristic island width associated with incomplete pressure flattening in the island and is determined by balancing time scales for cross-field transport $\chi_\perp$ across the island and low collisionality-convective transport parallel to the island,[8]

$$w_d\approx(RL_q\chi_\perp/nv_e)^{1/3}, \tag{2}$$

where $v_e=(2k_BT_e/m_e)^{1/2}$ is the local electron themal speed for temperature T_e. The choice of collisional parallel transport rather than convective would give a $w_d\propto(\chi_\perp/\chi_\|)^{1/4}$ scaling. The scaling for $\chi_\perp$ is uncertain and different transport models can result in different scalings of w_d, although the magnitude of w_d is relatively insensitive as $w_d\propto\chi_\perp^{1/3}$. In the thin island layer, the perpendicular diffusive transport is here taken as $\chi_{Bohm}=16^{-1}k_BT_e/eB_{\phi0}$, assuming the radial correlation length of turbulence is small compared to w. (With the island absent, the equilibrium transport is typically gyro-Bohm.) $B_{\phi0}$ is the axial toroidal magnetic field. The characteristic island w_d is evaluated to be small (<1 cm) and insignificant (compared with w_{pol} as discussed below) for existing devices[4,9] but is included in this work as potentially significant for reactor-grade tokamaks. Defining the dimensionless scaling parameter ρ_{i*} as ρ_i/a, where ρ_i is the ion gyroradius and a is the minor radius, the form for the relative size w_d/r can be written in terms of ρ_{i*} as

$$w_d/r\approx C_d\rho_{i*}^{1/3}, \tag{3a}$$

with a profile factor

$$C_d=\left[\frac{aR_0L_q}{32nr^3}\left(\frac{m_e}{m_i}\right)^{1/2}\right]^{1/3}. \tag{3b}$$

As a reactor-grade tokamak will have smaller ρ_{i*} than existing tokamaks, w_d/r will also be smaller.

The other moderating effect on the perturbed bootstrap current term of Eq. (1) is the helical polarization current arising from inertial effects.[10] Here, the characteristic island w_{pol} is of order of the ion banana width $\epsilon^{1/2}\rho_{\theta_i}$,

$$w_{pol}\approx g^{1/2}(\nu,\epsilon)(L_q/L_p)^{1/2}\epsilon^{1/2}\rho_{\theta_i}, \tag{4}$$

and has two regimes of collisionality: low with $\nu\equiv\nu_i/\epsilon\omega\ll1$ and $g(\nu,\epsilon)\equiv1$, and high with $\nu=\nu_i/\epsilon\omega\gg1$ and $g(\nu,\epsilon)=\epsilon^{-3/2}\gg1$, where $\rho_{\theta_i}\equiv v_i/(eB_\theta/m_i)$ is the poloidal ion gyroradius, ν_i is the ion collision frequency (to be discussed later), and ω is the propagation frequency of the mode in the $E\times B$ rest frame. Experiment (and theory) suggests $\omega\sim\omega_*$, the diamagnetic frequency, and which in our modeling we take as $\omega\sim\omega_{e*}=mT_e/rB_{\phi0}L_{pe}$, the local electron drift frequency for mode m with $L_{pe}=-p_e/(dp_e/dr)$ the electron pressure gradient scale length. w_{pol} is evaluated as 2–3 cm in existing devices in the low collisionality regime as compared to w_d of ~0.5 cm. The scaling of the relative size w_{pol}/r can be written in terms of the dimensionless size ρ_{i*} and the dimensionless collisionality ν as

$$w_{pol}/r\approx C_p\rho_{i*}g^{1/2}(\nu,\epsilon), \tag{5a}$$

with a profile factor

$$C_p=\left(\frac{\epsilon L_q a^2B_{\phi0}^2}{r^2L_pB_\theta^2}\right)^{1/2}, \tag{5b}$$

where B_θ is the local poloidal magnetic field. Note that the linear scaling of w_{pol}/r with ρ_{i*} is unfavorable for reactor-grade tokamaks and that ν scales as ν_*/ρ_{i*}, where ν_* is the more conventional definition of collision frequency, normalized to the trapped ion bounce frequency: $(\nu_i/\epsilon)/\omega_{bi}$ with $\omega_{bi}=\epsilon^{1/2}v_i/qR_0$ the ion trapped particle bounce frequency. For reactor-grade tokamaks, both ρ_{i*} and ν_* will be small compared to existing tokamaks but the ratio proportional to ν will be comparable to that presently obtained.

C. Critical beta scaling with seed island

Given the values of $\Delta' r$, w_{pol}/r, and w_d/r, etc., the marginal stability condition $dw/dt=0$ for the modified Rutherford equation (1) generally yields two branches: (a) a critical island width which the seed island must exceed to trigger the instability and (2) a saturated island width w_{sat}. This marginal stability curve in β_θ versus w space can be written as

$$\beta_\theta=A_0\left(\frac{w_{pol}}{r}\right)\left[\frac{w/w_{pol}}{1-(w_{pol}/w)^2}\right], \tag{6a}$$

for a profile factor A_0, assuming $w_{pol}^2\gg w_d^2$; the solution is shown in Fig. 1.

At $w=w_{min}=\sqrt{3}w_{pol}$, the marginal stability curve goes through a point where β_θ is a minimum,

$$\beta_{\theta,min}=\frac{3\sqrt{3}A_0}{2}\frac{w_{pol}}{r}, \tag{6b}$$

with

$$A_0=-\Delta' r/(\epsilon^{1/2}L_q/L_p), \tag{6c}$$

and below this, all values of β_θ are stable to any size seed island. The minimum β_θ of Eq. (6b) represents a lower limit which is unfavorable for reactor-grade tokamaks as $\beta_{\theta,min}\propto w_{pol}/r\propto\rho_{i*}$ at fixed ν.[10] However, for $\beta_\theta>\beta_{\theta,min}$, the stability depends on the seed island size, w_{seed}, relative to w_{pol}.

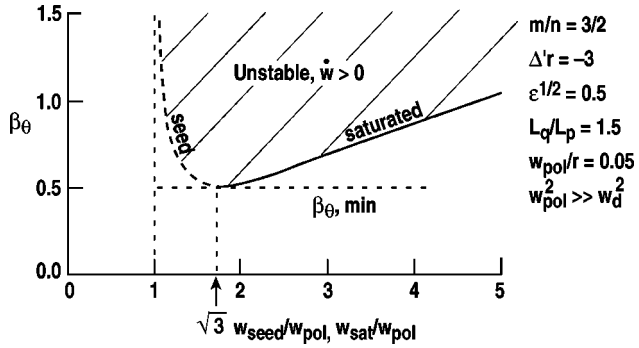

FIG. 1. β_θ versus w stability evaluated from the modified Rutherford equation. The unstable region is cross-hatched and is entered by crossing the dashed curve marked ''seed;'' this curve represents an unstable solution to the marginal stability equation. The seed island is then amplified to the solid curve marked ''saturated,'' which represents the stable solution to the marginal stability equation.

For $w_{\rm seed} \lesssim w_{\rm pol}$, all β_θ are stable as the seed cannot sufficiently disturb the metastable plasma. The unstable branch extends from $\beta_\theta = \infty$ at $w_{\rm seed}/w_{\rm pol} = 1$ to $\beta_\theta = \beta_{\theta,\rm min}$ for $w_{\rm seed}/w_{\rm pol} = \sqrt{3}$. The scaling to a reactor grade tokamak will thus depend on the scaling of the ratio of $w_{\rm seed}$ to $w_{\rm pol}$ (and perhaps to w_d, if significant). Consider a fixed ratio of $w_{\rm seed}/w_{\rm pol} > 1$, i.e., $w_{\rm seed}$ and $w_{\rm pol}$ have the same scaling, then $\beta_{\theta,\rm crit} > \beta_{\theta,\rm min} \propto w_{\rm pol}/r \propto \rho_{i*}$ at fixed ν. While there is no *a priori* reason for such a $w_{\rm seed}$ scaling, a roughly linear scaling of critical β_N with ρ_{i*} is observed experimentally with, in addition, a weaker ν scaling.[4,5,9] Here the more convenient choice of $\beta_N = \beta(\%)/(I_p/aB_{\phi 0})$ is used rather than β_θ with I_p, the plasma current in MA and $\beta_N \propto \beta_\theta$ for fixed shape and safety factor at the 95% poloidal flux within the separatrix boundary q_{95}.

D. Seed island dimensionless scaling

As the neoclassical tearing mode (NTM) critical beta depends on how the ratio of seed island to characteristic threshold islands scales, a model is needed for the dimensionless scaling of the seed island. It was pointed out in Ref. 4 that on DIII-D the $w_{\rm seed}$ measured from magnetic probe data analysis increases with ρ_{i*} and decreases with magnetic Reynolds number (Lundquist number) where

$$S \equiv \tau_R/\tau_A, \tag{7}$$

where $\tau_R = \mu_0 r^2/\eta$ is the local resistive diffusion time [1.22× that used in Eq. (1)] and $\tau_A = R_0(\mu_0 n_e m_i)^{1/2}/B_{\phi 0}$ is the ideal Alfvén time for local electron density n_e. The ρ_{i*} scaling, in hindsight, came from the range of $\sqrt{3} > w_{\rm seed}/w_{\rm pol} > 1$ needed for excitation, i.e., the data were only sampled when $w_{\rm seed} \sim w_{\rm pol} \propto \rho_{i*}$. This experimental result motivated theoretical considerations of the role of the dynamics of geometrically coupled perturbations.[11] Periodic sawteeth occur in which q on axis drops below unity, eventually leading to an explosively unstable $m/n = 1/1$ mode with an $m/n = 2/2$ harmonic and a periodic fast reconnection of the central flux raising q on axis above one. Toroidal effects at finite aspect ratio geometrically couple resonant perturbations between $q = m/n$ and $q = (m \pm 1)/n$ surfaces. The Shafranov shift $\Lambda(\beta_\theta)$ may also affect the geometric coupling at higher β_θ.[12] Thus a large $q = 1$ sawtooth instability can produce a small perturbation at $q = 3/2$. Dynamic shielding arises from a ''skin'' effect at the $q = 3/2$ singular surface which is analogous to a resistive wall and opposes the penetration of a rising radial magnetic field through induced eddy currents. The dynamic shielding factor is $S^{-\alpha}$, where $\alpha = 1/4 \sim 3/8$ depending on which physics assumptions are made. Note that another dynamic shielding factor $(\Delta\omega\tau_{\rm tear})^{-1/2}$ also exists where $\Delta\omega$ is the differential toroidal mode rotation between the $q = 1$ and $q = 3/2$ surfaces and the tearing time $\tau_{\rm tear} \approx \tau_R^{3/5}\tau_A^{2/5}$.[13] For DIII-D, for example, $(\Delta\omega\tau_{\rm tear})^{-1/2} \lesssim 25$, while $S^{3/8} \gtrsim 500$.

The relative seed island $w_{\rm seed}/r$ from coupling of $q = 1$ sawteeth to the $q = 3/2$ surface is represented as

$$\frac{w_{\rm seed}}{r} = \left(\frac{\tilde{\psi}}{\psi_0}\right)^{1/2} f\left(\frac{r_1}{R_0}, \frac{r_{3/2}}{R_0}, \Lambda\right) S^{-\alpha}, \tag{8a}$$

or

$$\frac{w_{\rm seed}}{r} = C_s \beta_\theta^\gamma S^{-\alpha}, \tag{8b}$$

where the strength of the perturbed flux at $q = 1$, $\tilde{\psi}/\psi_0$, and the geometric coupling factor are combined in C_s; β_θ^γ describes the increased coupling at higher β_θ, and $S^{-\alpha}$ describes the dynamic shielding at the $q = 3/2$ skin layer. Note that the value of α will be determined from the data shortly. To put Eq. (8b) in the dimensionless form in terms of ρ_{i*} and ν we rewrite S using Spitzer resistivity $\eta \equiv C_{\rm sp} T_e^{-3/2}$, ion collision frequency $\nu_i \equiv C_v n_e T_i^{-3/2}$, and $\beta_\theta = 2\mu_0 n_e k_B T/B_\theta^2$ with $T_e \approx T_i \equiv T$. Thus

$$S = C_S \beta_\theta^{1/2}/\rho_{i*}^3 \nu, \tag{9a}$$

with the profile factor

$$C_S = 2(B_\theta/B_{\phi 0})(L_{\rm pe} r^2/a^3) C_\nu m_i k_B^{3/2}/(C_{\rm sp} e^3). \tag{9b}$$

Note that at fixed β_θ and collisionality $\nu = \nu_i/\epsilon\omega_{e*}$, S rapidly increases with decreasing ρ_{i*} as one scales to a reactor-grade tokamak at low ρ_{i*}. Our final physics-based dimensionless scaling for $w_{\rm seed}/r$ (from $q = 1$ sawteeth inducing $q = 3/2$ NTMs only) is

$$\frac{w_{\rm seed}}{r} = C_s C_S^{-\alpha} \rho_{i*}^{3\alpha} \nu^\alpha \beta_\theta^{\gamma - \alpha/2} \equiv C_{s0} \rho_{i*}^{3\alpha} \nu^\alpha, \tag{10}$$

where, again, α is expected to be 1/4–3/8 depending on physics assumptions but will actually be fitted to the data. The parameter γ is chosen to be $\alpha/2$, consistent with data, such that $w_{\rm seed}/r$ is well behaved at low β_θ, i.e., $w_{\rm seed}/r$ would go to infinity at low β_θ for $\gamma < \alpha/2$, and to make the right-hand side (rhs) of Eq. (6a) independent of β_θ. Note that for the special case of $\alpha = 1/3$, $w_{\rm seed}/w_{\rm pol} = (C_s C_S^{-1/3} C_p^{-1}) \nu^{1/3}/g^{1/2}(\epsilon, \nu)$ is independent of ρ_{i*} and is a weak function of ν. This scaling (or $\alpha < 1/3$) would be unfavorable for a reactor-grade tokamak. A scaling $\alpha > 1/3$ is favorable, as at low enough ρ_{i*}, high enough S, the seed island may be too small due to dynamic shielding to disturb the metastable plasma.

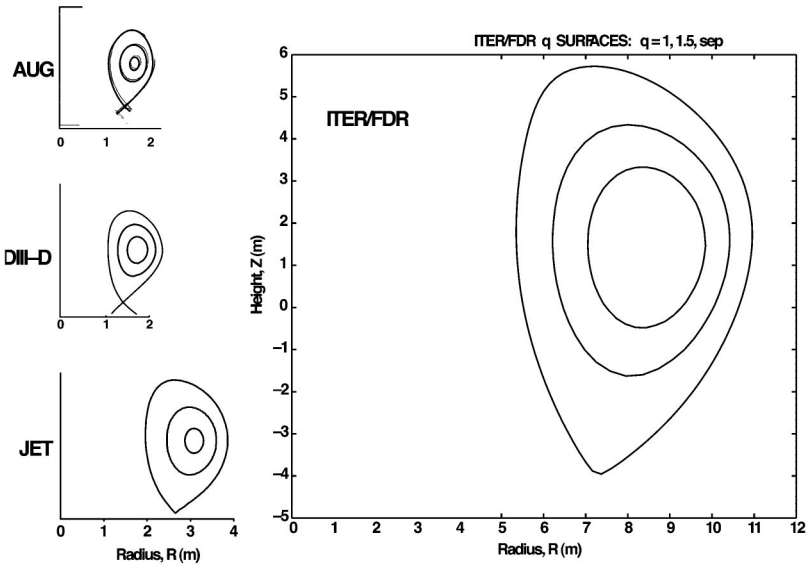

FIG. 2. Separatrix as well as $q=1$ and $q=3/2$ surfaces for (a) ASDEX Upgrade, (b) DIII-D, (c) JET, and (d) ITER/FDR, showing relative sizes.

E. Critical beta dimensionless scaling with the α parameter

The form for the critical beta, now including the incomplete pressure flattening threshold, is

$$\beta_{\theta,\mathrm{crit}}=A_0 C_p \rho_{i*} g^{1/2}(\nu,\epsilon) \times\left[\frac{\dfrac{(C_{s0}/C_p)\rho_{i*}^{3\alpha-1}\nu^{\alpha}}{g^{1/2}(\nu,\epsilon)}}{\left(1+\dfrac{C_d^2\rho_{i*}^{2/3-6\alpha}}{C_{s0}^2\nu^{2\alpha}}\right)^{-1}-\left(\dfrac{C_p^2 g(\nu,\epsilon)}{C_{s0}^2\rho_{i*}^{6\alpha-2}\nu^{2\alpha}}\right)}\right], \quad (11a)$$

with $g(\nu,\epsilon)=(1+C_2\nu)/(1+C_3\nu)$, and the numerical coefficients $C_2/C_3\approx\epsilon^{-3/2}$ model the transition from the low ν to the high ν polarization/inertial thresholds.[4,10] Consider the special case of $C_d\to 0$, $g(\nu,\epsilon)\to 1$, and $\alpha\equiv 1/3$. Then

$$\beta_{\theta,\mathrm{crit}}=A_0 C_p \rho_{i*}\left[\frac{(C_{s0}/C_p)\nu^{1/3}}{1-(C_p^2/C_{s0}^2)\nu^{-2/3}}\right], \quad (11b)$$

and the expected critical beta separates into a linear ρ_{i*} factor multiplied by a separable function of ν. When the denominator is close to unity, the function of ν will be weak, $\sim\nu^{1/3}$ for the low collisionality regime.

Next consider another special case of $C_d\to 0$, $g(\nu,\epsilon)\to 1$, but $\alpha\equiv 4/9$. Then

$$\beta_{\theta,\mathrm{crit}}=A_0 C_p \rho_{i*}^{4/3}\left[\frac{(C_{s0}/C_p)\nu^{4/9}}{1-(C_p^2/C_{s0}^2)(\nu^{-8/9}/\rho_{i*}^{2/3})}\right]. \quad (11c)$$

For $\alpha=4/9$, the ρ_{i*} and ν scalings are not separable. At fixed ν, two competing dependencies on ρ_{i*} exist. Lower ρ_{i*} decreases the characteristic polarization/inertial threshold; the numerator of Eq. (11c) becomes smaller. However, lower ρ_{i*}/higher S leads to a smaller seed island, tending to make the denominator smaller and $\beta_{\theta,\mathrm{crit}}$ higher. For this special case with $\alpha=4/9$, Eq. (11c) has a value of ν that minimizes $\beta_{\theta,\mathrm{crit}}$ which depends on ρ_{i*},

$$\nu_{\min}=(3C_p^2/C_{s0}^2)^{9/8}\rho_{i*}^{-3/4}. \quad (12)$$

Again assuming $C_d=0$, $g(\nu,\epsilon)\equiv 1$, and $\alpha\equiv 4/9$, $\beta_{\theta,\mathrm{crit}}$ will increase weakly with collisionality ν for $\nu>\nu_{\min}$ and increase with decreasing ν for $\nu<\nu_{\min}$. From Eq. (12), one expects that for $\alpha=4/9$, the value of $\nu_{\min}$ where $d\beta_\theta/d\nu$ changes sign will shift to higher collisionality for lower ρ_{i*}-higher S.

While this analysis can be generalized for any regime and α starting from Eq. (11a), one predicts from the model: (1) for $\alpha=1/3$, a separable critical β_θ of nearly linear ρ_{i*} times a function of collisionality ν, i.e., the ratio of $\beta_{\theta,\mathrm{crit}}$ to ρ_{i*} will be independent of ρ_{i*}, (2) for $\alpha>1/3$, the dependence of $\beta_{\theta,\mathrm{crit}}$ on ρ_{i*} and ν is not separable, i.e., the dependence of $\beta_{\theta,\mathrm{crit}}/\rho_{i*}$ with ν will change as ρ_{i*} is scanned.

III. EXPERIMENTAL DESCRIPTION AND DATABASE

A. Configuration

In order to study the scaling of the NTM threshold over a wide range of parameters, a database was compiled from a number of tokamaks. The discharges studied are ELMy (with edge localized modes) H-mode lower single-null divertor (SND) at a safety factor $q_{95}=3.2-3.5$ at the 95% poloidal flux surface within the separatrix. Elongation and lower triangularity at the separatrix are $\kappa\approx 1.7$ and $\delta\approx 0.4$, respectively. Inverse aspect ratio is $a/R_0\approx 0.35$. Periodic $q=1$ sawteeth are observed to induce $m/n=3/2$ NTMs in the discharges considered from ASDEX Upgrade,[3] DIII-D,[4] and JET,[5] and all evaluations of ρ_{i*}, ν, and β_N are made just before onset of such a mode. The plasma shapes and relative sizes are shown in Fig. 2. The regimes of discharges considered for this study are chosen to match that for the ITER/FDR reactor-grade tokamak design also shown to scale in Fig. 2. All discharges are neutral beam heated, D_2, and $T_i\approx T_e$. By fixing shape, q_{95}, κ, δ, and the sawteething, ELMy H-mode regime, it is anticipated that current, q, and p profiles will be similar from device to device. On DIII-D, for example,[4] there is considerable ''profile consistency'' as power, field, and density are varied at constant shape, q_{95},

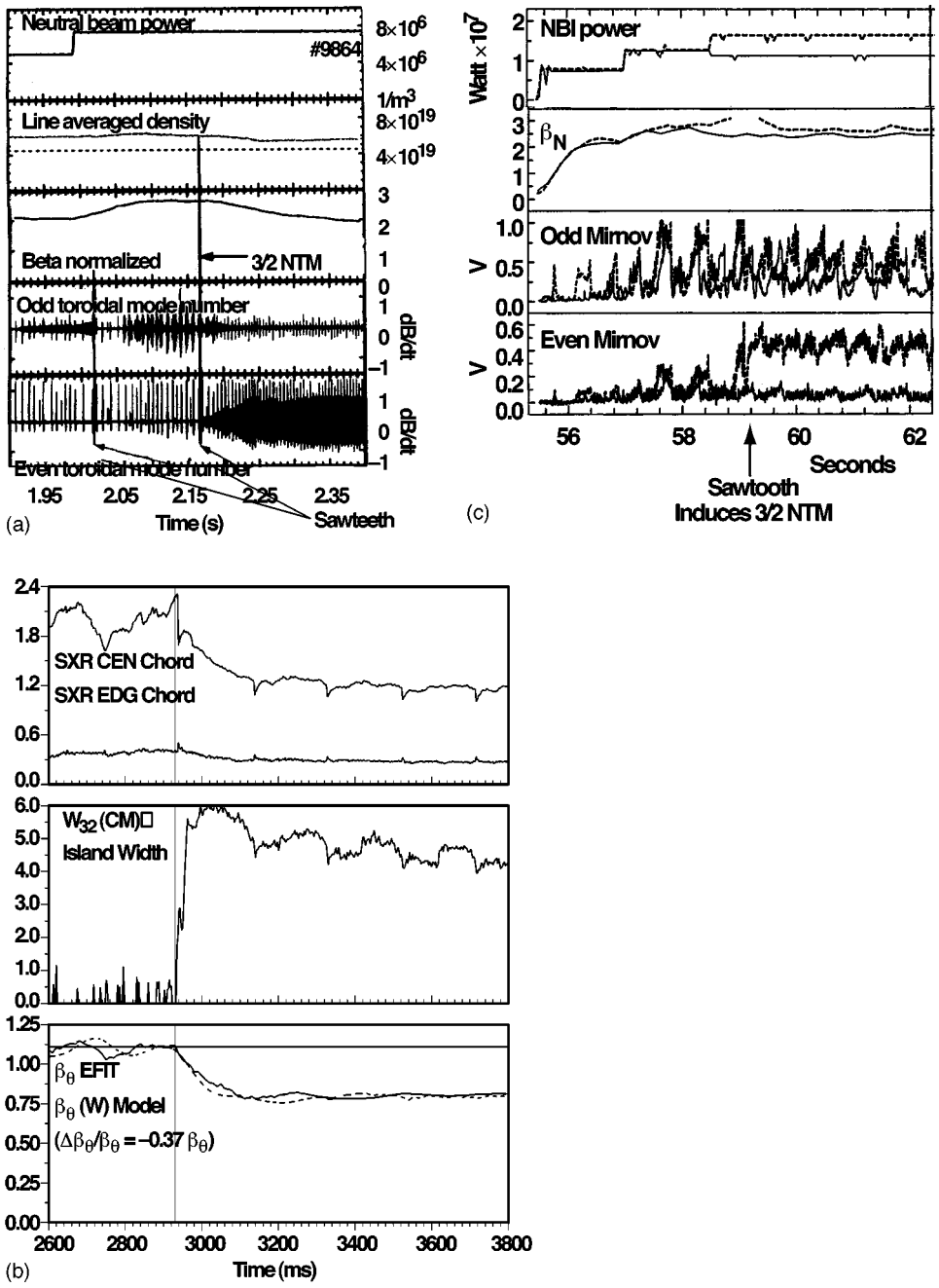

FIG. 3. (a) ASDEX Upgrade: neutral beam power, line averaged density, β_N, odd toroidal mode number Mirnov activity dB/dt, even toroidal mode number, Mirnov activity dB/dt showing 3/2 mode after sawtooth and drop in β_N. (b) DIII-D: central and edge soft x-ray chords, $m/n=3/2$ island width (calculated from Mirnov data $w \propto \tilde{B}_\theta^{1/2}$) and beta poloidal calculated from MHD reconstruction code EFIT. The neutral beam power was stepped up just before the time trace starts and the fitted $\beta_\theta(w)$ is from the Chang and Callen ''belt'' model. (c) JET: NBI power, β_N, odd Mirnov (dB/dt) and even Mirnov (dB/dt) for two discharges, (1) solid line has no final step up in power and despite periodic sawtooth (jumps on odd Mirnov) remains stable to 3/2 NTM, (2) dashed line has extra step up in power, initially higher β_N but 3/2 NTM excited on sawtooth reduces β_N almost down to that of the discharge with lower power.

and regime (sawteething, ELMy H-mode) with the local electron and ion temperature radial gradient scale lengths L_{T_e} and L_{T_i} comparable and the electron density radial gradient scale length L_{n_e} about 3.5 times L_{T_e} or L_{T_i}.

A number of other tokamaks which have also experienced neoclassical tearing modes are not included in this study. For reasons of shape (circular-limited) and regime (''supershot''), Tokamak Fusion Test Reactor (TFTR) is not included.[2] While the COMPASS-D tokamak does have the appropriate shape and regime [except for $T_e \gg T_i$ as electron cyclotron resonant heating (ECH) is used], $m/n=2/1$ NTMs are observed at high heating power, while $m/n=3/2$ NTMs are not.[14] This may be related to the use of ECH in very low density plasmas, resulting in the observed very centrally peaked T_e and low T_i. Plans to study NTMs on Alcator C-Mod, which would be of considerable interest due to its very high toroidal field, await sufficient additional heating power to access high β_N.[15] Finally, while NTMs are observed on Japan Torus-60 Upgrade (JT-60U), and are of considerable scaling interest due to having both high field and large size, sawteeth and $q(0)=1$ disappear in long-pulse high beta discharges.[16,17] Future contributions from Alcator C-Mod and JT-60U should provide an opportunity to test the predictions from the model fitted in Sec. IV.

B. Examples of $q=1$ sawteeth inducing $m/n=3/2$ NTMs

All cases studied here are of discharges with slowly rising beta where a $q=1$ sawtooth crash induces the $m/n=3/2$ NTM. Often the first ''limit'' on beta and confinement,

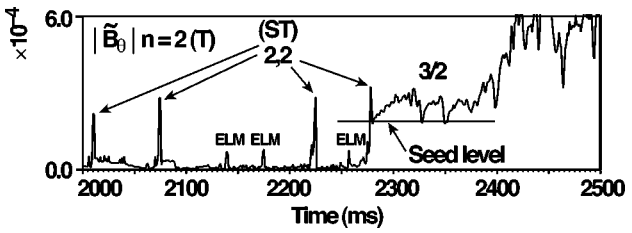

FIG. 4. $n=2$ Mirnov amplitude $\tilde{B}_\theta$ versus time in DIII-D. Peaks for sawteeth (ST) and ELMs are noted as well as ''seed level'' after the ST that induces a growing $m/n=3/2$ NTM.

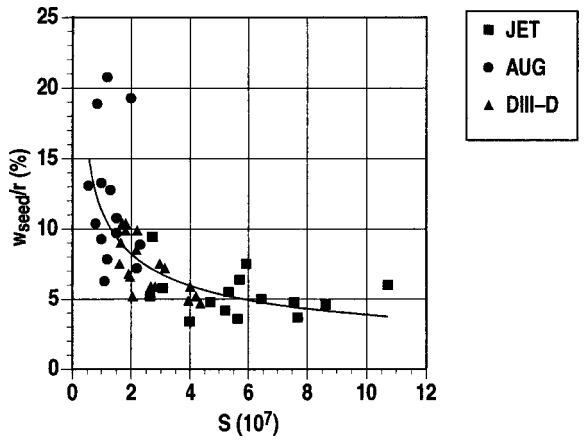

FIG. 5. Scaling of relative seed island w_{seed}/r (in %) versus magnetic Reynolds number S (at $q=3/2$ in units of 10^7). Best fit is $w_{\text{seed}}/r(\%) = 11.3S^{-0.46\pm0.05}$ with correlation $=-0.74$.

this mode can cause beta (at fixed input power) to drop by 10%–30%. A case for ASDEX Upgrade is shown in Fig. 3(a),[3,18] for DIII-D in Fig. 3(b),[4,19,20] and for JET in Fig. 3(c).[5] While not exactly comparable figures, Figs. 3(a), 3(b), and 3(c) give the flavor of the effect seen.

Note that the critical beta for onset of $m/n=3/2$ NTMs discussed in this work is not actually a beta ''limit.'' After exciting a 3/2 NTM and subsequent confinement degradation, which is well described by the Chang and Callen ''belt'' model,[3,19,20] adding additional power can increase beta back to or above the critical value.[21,22] This is a ''soft'' limit as $w_{\text{sat}} \propto \beta_\theta$ and $\Delta\beta_\theta/\beta_\theta \propto -w_{\text{sat}} \propto -\beta_\theta$, so as β_θ is increased, the island expands, further degrading the confinement. The ultimate ''hard'' NTM limit is observed when the $m/n=2/1$ mode is excited, usually following the 3/2 NTM in these ITER/FDR regime discharges; this mode has a larger associated confinement reduction and often leads to loss of H-mode and disruption.[5,21,22]

C. Seed island scaling with magnetic Reynolds number *S*

A key ingredient in the critical beta scaling is how the seed island scales. The seed island scaling model [Eqs. (7)–(10)] is found to be consistent with the multidevice database. Here the island width is determined from the Mirnov data, where available, with correction using electron cyclotron emission (ECE) measurements.[2,4,23–25] A toroidal array of Mirnov probes on the outboard midplane is used to measure dB_θ/dt. The integrated $\tilde{B}_\theta$ amplitude for the $n=2$ signal is shown versus time for an example from DIII-D in Fig. 4. The value of $\tilde{B}_\theta$ that grows after a sawtooth is taken as the ''seed level.'' This is converted into a radial field at the $q=3/2$ minor radius r (at the outboard midplane) as

$$|\tilde{B}_r| \approx \frac{1}{2}\left(\frac{b}{r}\right)^4 |\tilde{B}_\theta|_{\text{wall}}, \tag{13a}$$

where the probe is at minor radius b and $m+1=4$ for the assumed $m=3$. This $|\tilde{B}_r|$ is then used to determine the seed island width through

$$w_{\text{seed}} \approx \left(\frac{16 r R_0 |\tilde{B}_r|}{3 s B_{\phi 0}}\right)^{1/2}, \tag{13b}$$

where $s=r(dq/dr)/q^2$ with $q=3/2$.

For multidevice comparison, the magnetohydrodynamic (MHD) equilibrium reconstruction code ''EFIT'' is used to find the major radii of the $q=3/2$ surface R_{in} and R_{out} on the midplane. The $q=3/2$ minor and major radii are then defined as $r=(R_{\text{out}}-R_{\text{in}})/2$ and $R_0=(R_{\text{out}}+R_{\text{in}})/2$, respectively. The shear s is taken assuming $q \equiv 0.9+(q_{95}-0.9)r^2/a^2$ just before the sawtooth crash. Applying Eq. (13) to shaped finite aspect ratio discharges leads to a systematic error which is corrected by comparison to direct outboard midplane island measurements of large, saturated islands (after 2500 ms in Fig. 4, for example) by fast ECE radiometer. This measurement indicates that the w_{seed} from Eq. (13) must be corrected by a factor of 1.31, 0.68, and 0.60, respectively, for ASDEX Upgrade, DIII-D, and JET. This ECE measurement also has an uncertainty due to the finite radial channel spacing ($\Delta R \approx 2$ cm on DIII-D) and bandwidth. The large saturated island width measured from ECE at 6.5 cm (corresponding to $w_{\text{sat}}/r \approx 15\%$) on DIII-D which was used to get the factor 0.68 correction of the Mirnov estimated island is thus itself uncertain. Given this, the ECE corrected w_{seed}/r from Mirnov data are adjusted by factors of 0.80, 1.00, and 0.70, respectively, for ASDEX Upgrade, DIII-D, and JET to maximize the correlation of w_{seed}/r versus S as shown in Fig. 5. The best fit has $w_{\text{seed}}/r = 11.3(\%)S^{-0.46\pm0.05}$ with correlation -0.74. Here S is evaluated at the $q=3/2$ outboard midplane location using Thomson scattering for T_e and n_e and $\eta \equiv 7.8\times10^{-4}T_e^{-3/2}$(eV) with $Z_{\text{eff}} \equiv 1$. Some of the larger w_{seed}/r data points in Fig. 5 do not actually grow after excitation and thus may be at the knee of the curve in Fig. 1.

Actually, the ''seed levels'' measured in this manner must exceed the threshold in order for the NTM to grow. The critical β fitting, to be described later, must also make the assumption that the onset of NTM growth is just at the seed curve of Fig. 1 or has not exceeded it by much. Careful control of all discharges in the database was used to raise beta on a time scale slower than that of the sawtooth period so as to make this onset condition close to the seed curve. However, variations in sawteeth, etc., will introduce an unavoidable scatter in the data. Thus the levels of w_{seed}/r, and of critical beta to be described next, tend to be overestimates.

D. Critical beta scaling with collisionality and normalized gyroradius

The database is based on a dimensionless collision frequency ν and a dimensionless size ρ_{i*}. Both $\nu=\nu_i/\epsilon\omega_{e*}$ and ρ_{i*} are evaluated at the $q=3/2$ outboard midplane location. The ion collision frequency from Thomson scattering and charge exchange spectroscopy data is $\nu_i=5.09\times10^{-7}n_e\,(\mathrm{cm}^{-3})/T_i^{3/2}\,(\mathrm{eV})$ for $Z_{\mathrm{eff}}\equiv1$. The local inverse aspect ratio is $\epsilon=r/R_0$ where r and R_0 are defined in Sec. III C. The electron drift frequency is $\omega_{e*}=mT_e/rL_{\mathrm{pe}}B_{\phi0}$, with $m\equiv3$ and $L_{\mathrm{pe}}=-p_e/(dp_e/dR)$ the electron pressure gradient scale length. While careful attention to spatial and temporal fitting is made to measure L_{pe}, this gradient does introduce scatter into the collisionality with ν. The values of normalized Larmor radius, ρ_{i*}, are much less sensitive to fitting and are taken as $\rho_{i*}=[m_i(2k_BT_i/m_i)^{1/2}/eB_{\phi0}]/a$ using the axial $B_{\phi0}$. All cases studied are in deuterium with $m_i=2m_p$, m_p being the proton mass. The multidevice database has $\nu=0.01$ to 0.14 and $\rho_{i*}=5\sim12\times10^{-3}$. A typical ITER/FDR[6] case for $\beta_N=2.5$ and Greenwald density $G=n_{14}\pi a^2/I_p(\mathrm{MA})=1.35$ has $\nu=0.13$ and $\rho_{i*}=1.2\times10^{-3}$.[14] Note that as $\nu\propto\nu_*/\rho_{i*}$, the existing tokamaks cover the range of $\nu=\nu_i/\epsilon\omega_{e*}$ expected for ITER/FDR despite its smaller expected ν_* and ρ_{i*}.

A test of whether the critical beta can be expressed as a separable function, i.e., $\beta_N\propto f(\rho_{i*})h(\nu)$, is shown in Fig. 6(a). While ASDEX Upgrade and DIII-D are similar to each other and have positive power law dependence with ν, fixing a linear ρ_{i*} scaling ($\beta_N/\rho_{i*}=5.8\nu^{0.25}$ and $9.4\nu^{0.43}$, respectively), JET has a much weaker negative power law dependence with ν ($\beta_N/\rho_{i*}=2.6\nu^{-0.08}$). The different ν scaling of β_N/ρ_{i*} lets us immediately state that a separable scaling is not appropriate to fit the data and that $\alpha\neq1/3$ in our model. [See Eq. (11b). This presumes that the w_d term of Eq. (11a) is negligible as will be shown later in the complete fit.] As β_N/ρ_{i*} is higher for JET at low ν, and has weaker dependence on ν, this suggests that for the lower ρ_{i*} [see Fig. 6(b)], higher S, JET, the $\nu_{\min}$ from Eq. (12) has shifted lower, consistent with $\alpha>1/3$ and Eq. (11c) ($\alpha\equiv4/9$). This anticipates the fit for α which will be made later. The plot of β_N normalized by the best $f(\nu)$ solid lines of Fig. 6(a) is shown versus ρ_{i*} in Fig. 6(b). The factor of 3 comes from the approximate crossing of the solid curves in Fig. 6(a) at $\beta_N/\rho_{i*}\approx3$ for $\nu=0.08$. While the linear dependence on ρ_{i*} in Fig. 6(b) provides strong supporting evidence for the polarization/inertial threshold model, Eqs. (5a), (6c), and (11b), the different ν scalings (even the sign of the power) make this an incomplete model for extrapolation to ITER/FDR, for example. For contrast, free empirical fits are given in Table I. All three devices, taken separately, have nearly linear ρ_{i*} scaling. While AUG and DIII-D go well together with a standard deviation little different than taken individually, all devices taken together have a reduced chi squared about four times larger, and a weak ρ_{i*} scaling. Again, clearly, the larger JET is in a different regime than the closer together in size AUG and DIII-D.

Taking the assumptions used to derive Eq. (11c), there is a value of ρ_{i*} that minimizes $\beta_{\theta,\mathrm{crit}}$, using an argument similar to that for Eq. (12) of

$$\rho_{i*,\min}=(3C_p^2/2C_{s0}^2)^{3/2}\nu^{-4/3}, \tag{14a}$$

for the special case of $\alpha\equiv4/9$ and $w_d\equiv0$. Thus at fixed ν one expects a $\beta_{\theta,\mathrm{crit}}\propto\rho_{i*}^{4/3}$ (i.e., nearly linear) for $\rho_{i*}\gg\rho_{i*,\min}$, no dependence of $\beta_{\theta,\mathrm{crit}}$ on ρ_{i*} for $\rho_{i*}\approx\rho_{i*,\min}$ and an *increasing* $\beta_{\theta,\mathrm{crit}}$ with *decreasing* ρ_{i*} for $\rho_{i*}<\rho_{i*,\min}$, with stability for $\rho_{i*}\leqslant\rho_{i*,\mathrm{stable}}$ where

$$\rho_{i*,\mathrm{stable}}=(C_p^2/C_{s0}^2)^{3/2}\nu^{-4/3}. \tag{14b}$$

Note that $\rho_{i*,\mathrm{stable}}\approx0.2\rho_{i*,\min}$ if $\alpha\equiv4/9$ and the w_d/r term is neglected. Including the incomplete pressure flattening threshold can raise $\rho_{i*,\min}$ as will be seen later.

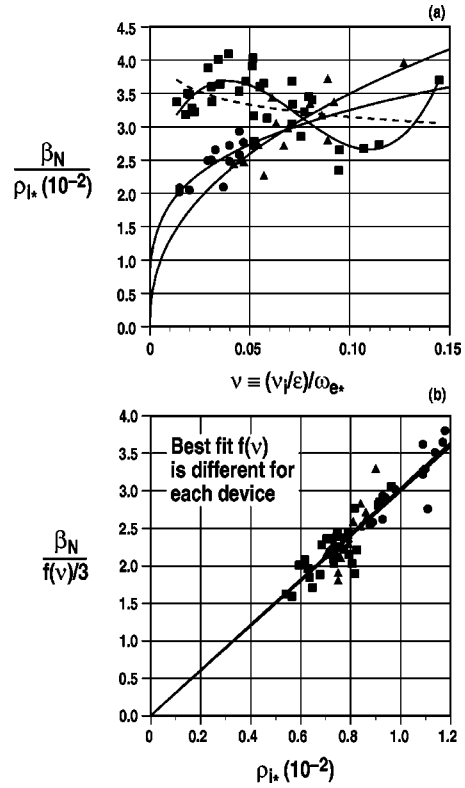

FIG. 6. (a) Ratio of critical beta to normalized ion gyroradius versus collisionality. ■ JET, ● ASDEX Upgrade, ▲ DIII-D. Solid lines for ASDEX Upgrade and DIII–D are best power law fits, solid line for JET is best third order polynomial fit, while dashed line is best power law fit. (b) Same data plot with ratio of critical beta normalized by best fit function of collisionality versus rhoistar (ρ_{i*}). Note that $f(\nu)$ is different for each device and the factor of 3 included in the normalization allows for where the best fit curves cross (a). ■ JET, ● ASDEX Upgrade, ▲ DIII-D.

TABLE I. Free empirical fits to $\beta_N=C(\rho_{i*}/10^{-2})^x(\nu_i/\epsilon\omega_{e*})^y$ (σ_{β_N} is the standard deviation of the experimental and fitted critical β_N).

Device	# Data	C	x	y	σ_{β_N}
AUG	14	5.7	1.1	0.25	0.20
DIII-D	15	9.6	1.3	0.43	0.22
JET	33	2.2	0.64	−0.10	0.29
AUG & DIII-D	29	7.3	1.2	0.32	0.23
All	62	2.7	0.41	0.00	0.38

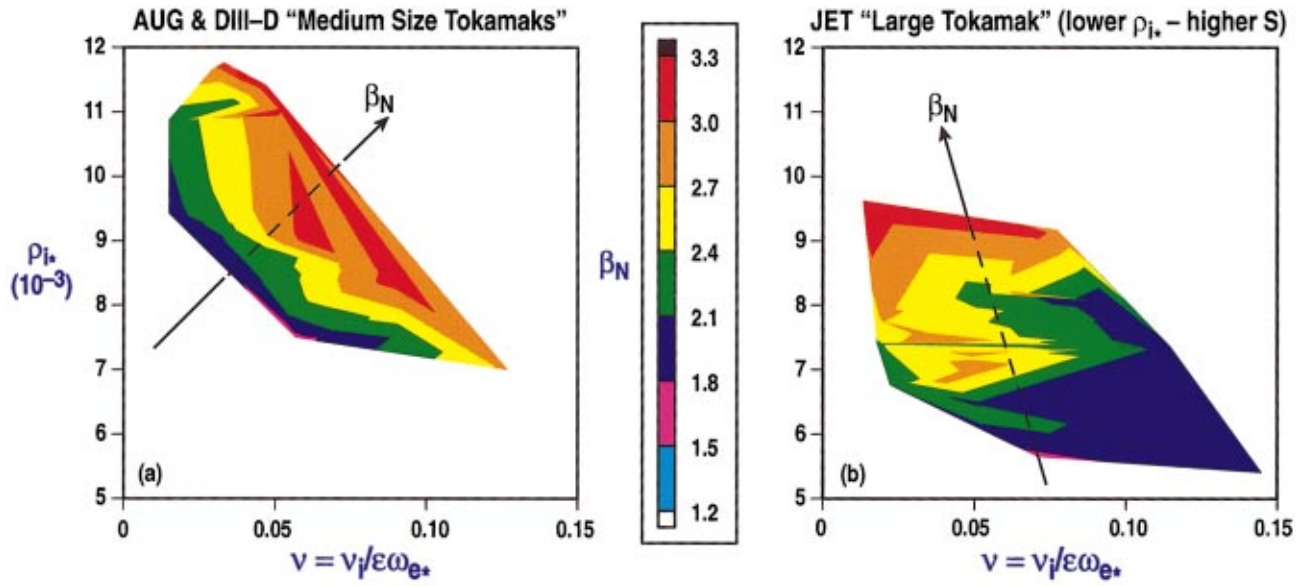

FIG. 7. (Color) Contour plots of critical β_N data for $q=1$ sawtooth induced $m/n=3/2$ NTM in ρ_{i*}, ν space. Each β_N contour is 0.3 wide. (a) ''Medium-size tokamaks'' ASDEX Upgrade, and DIII-D, arrow is $\beta_N \propto \rho_{i*}\nu^{0.3}$. (b) ''Large-size tokamak'' JET, arrow is $\beta_N \propto \rho_{i*}\nu^{-0.1}$.

The β_N, ρ_{i*}, ν data from Fig. 6 are shown in contour plots in Fig. 7. ASDEX Upgrade and DIII-D are combined in Fig. 7(a) and show an increasing critical beta with larger ρ_{i*} and greater collisionality. JET stands alone in Fig. 7(b) and again shows an increasing critical beta with larger ρ_{i*} but β_N weakly decreasing with greater collisionality. Reiterating, the difference in ν-scaling implies a lack of separability of the ρ_{i*} and ν scalings and thus an $\alpha \neq 1/3$ dependence of the relative seed island with magnetic Reynolds number. The change in the power of the ν scaling between AUG/DIII-D and JET from positive to negative is consistent with Eqs. (11c) and (12); at the lower ρ_{i*}, higher S in JET, the variation in $w_{\text{seed}}/w_{\text{pol}}$ becomes more significant, i.e., the denominator in Eq. (11c), for $\beta_{\theta,\text{crit}}$, determines the ν-scaling. While ASDEX Upgrade and DIII-D are in the regime where $\beta_{\theta,\text{crit}}$ increases with increasing threshold, JET has entered the regime where $\beta_{\theta,\text{crit}}$ increases with decreasing seed island.

IV. MULTIPARAMETER CRITICAL BETA FIT

The database for $q=1$ sawtooth induced $m/n=3/2$ NTMs in AUG, DIII-D, and JET in regimes similar to that expected for ITER/FDR is fitted to our model, which can be expressed in terms of ρ_{i*} and ν as

$$\beta_{\text{NC}} = \frac{C_0 C_1 \rho_{i*}^{3\alpha} \nu^{\alpha}}{\dfrac{1}{1+C_4^2 \rho_{i*}^{2/3-6\alpha_\nu-2\alpha}} - \dfrac{(1+C_2\nu)/(1+C_3\nu)}{C_1^2 \rho_{i*}^{6\alpha-2} \nu^{2\alpha}}}, \quad (15)$$

with ρ_{i*} in units of 1×10^{-3}. The parameters to be fitted are C_0, C_1, C_2, C_3, C_4, and α. Thus, Eq. (15) can be compared to Eq. (11). The overall constant of proportionality $C_0 = 10^{-3}(\beta_N/\beta_\theta)A_0 C_p$ with $A_0 = -\Delta' r/(\epsilon^{1/2} L_q/L_p)$ from Eq. (6b) and C_p from Eq. (5b). This incorporates various profile factors which are expected to be similar for this database. While individual discharge profiles are used to evaluate ρ_{i*} and ν, C_0 will be proportional to a mean value of $\Delta' r$.[26] $C_1 = (1\times10^{-3})^{3\alpha-1} C_{s0}/C_p$ from Eqs. (5b), (8b), (9a), (9b), and (10) represents the constant of proportionality for the relative size of the seed island to the polarization/inertial characteristic island. C_2 and C_3 represent the transition of the polarization/inertial characteristic island from collisionless $\nu \ll C_2^{-1}$ with $g(\epsilon,\nu)=1$ to collisional with $\nu \gg C_2^{-1}$ and $g(\epsilon,\nu) \approx C_2/C_3 = O(\epsilon^{-3/2} \gg 1)$. $C_4 = C_d/C_{s0}$ from Eqs. (3b), (8b), (9a), (9b), and (10) represents the constant of proportionality of the relative size of the incomplete pressure flattening characteristic threshold island to that of the seed island. Finally, α is the key parameter for the $w_{\text{seed}}/r \propto S^{-\alpha}$ dynamic coupling model.

In order to scale Eqs. (14) and (15) to a reactor-grade tokamak, such as ITER/FDR, the best fitted values for $C_0, \ldots, C_4$ and α are made from the ASDEX Upgrade, DIII-D, JET database by minimizing

$$\chi^2 \equiv \frac{1}{N-n-1} \sum_1^N w_i [\beta_{N,\text{data}} - \beta_{N,\text{model}}]_i^2, \quad (16)$$

where there are $N=62$ data points and $n+1=6$ fitted constants. The weights w_i for the data from each device are determined iteratively from the variance σ_{β_N} of the fit evaluated for each device first with all $w_i \equiv 1$, then refitted with $w_i \sim \sigma_{\beta_N}^{-2}$ such that $\Sigma w_i \equiv N$ data points. The final weights used are $w_i = 0.70$ for JET and 1.34 for ASDEX Upgrade and DIII-D. The overall $\sigma_{\beta_N} = 0.37$ compared to $\sigma_{\beta_N} = 0.20$ for ASDEX Upgrade, 0.25 for DIII-D, and 0.31 for JET from the separate best fit curves of Fig. 6(b). In performing the fitting, a test is made of each case to check if it is on the ''seed'' curve of Fig. 1; if found on the ''saturated'' curve of Fig. 1, the fitted β_N is set to the minimum value consistent with Eq. (6b).

The significance of each of the best fit constants will be evaluated for typical data values of $\nu = 0.075$ and $\rho_{i*} = 7.0$

TABLE II. Best fit constants and consequences (typical database has values of $\rho_{i*}=7.0\times10^{-3}$ and $\nu=0.075$; ITER/FDR has $\rho_{i*}=1.2\times10^{-3}$ and $\nu=0.13$).

Parameter	Best fit	Database consequences	ITER/FDR consequences
C_0	0.057	$\Delta' r\approx-3.1$	same
C_1	5.95	$w_{seed}/w_{pol}\approx1.8$ (large enough for NTM)	$w_{seed}/w_{pol}=1.0$ (marginally too small for NTM excitation)
C_2, C_3	56.5,3.1	$\nu_{low}\leqslant0.02$, $\nu_{high}\geqslant0.32$, $(C_2/C_3)^{1/2}=4.2$ compared to $\epsilon^{-3/4}\approx3.3$ from large aspect ratio tokamak theory	same
C_4	0.60	$w_d/w_{seed}\approx0.26$, $w_{pol}^2=4.4w_d^2$, $w_{seed}/(w_{pol}^2+w_d)^{1/2}\approx1.6>1$	$w_d/w_{seed}\approx1.3$, $w_{pol}^2=0.6w_d^2$ $w_{seed}/(w_{pol}^2+w_d^2)^{1/2}\approx0.6<1$
α	0.46±0.08	$w_{seed}/w_{pol}\propto\rho_{i*}^{0.38\pm0.24}$ at fixed ν	same

$\times10^{-3}$. See Table II. $C_0=0.057$ yields a typical value of $\Delta' r=-3.1$ for $\beta_\theta/\beta_N=1/3$, $B_\theta/B_{\phi0}=1/5$, $\epsilon=1/5$, $L_q/L_p=1.5$, and $r/a=0.65$. This is a value in the midrange between marginally stable, $\Delta' r=0$, and very stable, $\Delta' r\approx-2m=-6$, current profiles. $C_1=5.95$ (with $\alpha=0.46$, $C_2=56.5$, and $C_3=3.1$) yields a ratio of w_{seed} to w_{pol} of 1.8 for the typical data value ($\nu=0.075$ and $\rho_{i*}=7.0\times10^{-3}$) and 1.0 for ITER/FDR ($\nu=0.13$ and $\rho_{i*}=1.2\times10^{-3}$). Thus the existing NTM unstable discharges are fitted by seed islands exceeding the polarization/inertial threshold. Using the model to extrapolate to the ITER/FDR suggests its seed islands would be too small to excite the NTM based on the polarization/inertial threshold *alone*.

The fitted parameters $C_2=56.5$ and $C_3=3.1$ for the collisionality dependence of the polarization/inertial threshold are equivalent to: (1) the low collisionality regime is entered for $\nu\leqslant C_2^{-1}=0.02$, (2) the high collisionality regime is entered for $\nu\geqslant C_3^{-1}=0.32$, therefore most of the existing data (and ITER/FDR) are in the transition regime, (3) $C_2/C_3=18$ compared to a predicted, large aspect ratio tokamak estimate of $\epsilon^{-3/2}\approx11$, thus the high collisionality polarization/inertial threshold island would, if accessed, be a factor of $18^{1/2}\approx4$ times higher than that for the low collisionality regime. Operation at very high field, and hence low ρ_{i*}, may allow this regime to be accessed.

The parameter $C_4=0.60$ (with $\alpha=0.46$) which characterizes the incomplete pressure flattening threshold yields a relative w_d characteristic island size to that of w_{seed} of 0.26 for typical data values ($\rho_{i*}=7.0\times10^{-3}$ and $\nu=0.075$) and 1.3 for ITER/FDR ($\rho_{i*}=1.2\times10^{-3}$ and $\nu=0.13$). Thus for the typical values of existing devices: (1) $w_{pol}^2\approx4.4w_d^2$ and the polarization/inertial threshold dominates over the incomplete pressure flattening threshold, (2) the ratio of w_{seed} to the effective characteristic threshold island size $(w_{pol}^2+w_d^2)^{1/2}$ is about 1.6, and (3) the first term in the denominator of the critical beta model Eq. (14) is about 0.94 or close to unity.

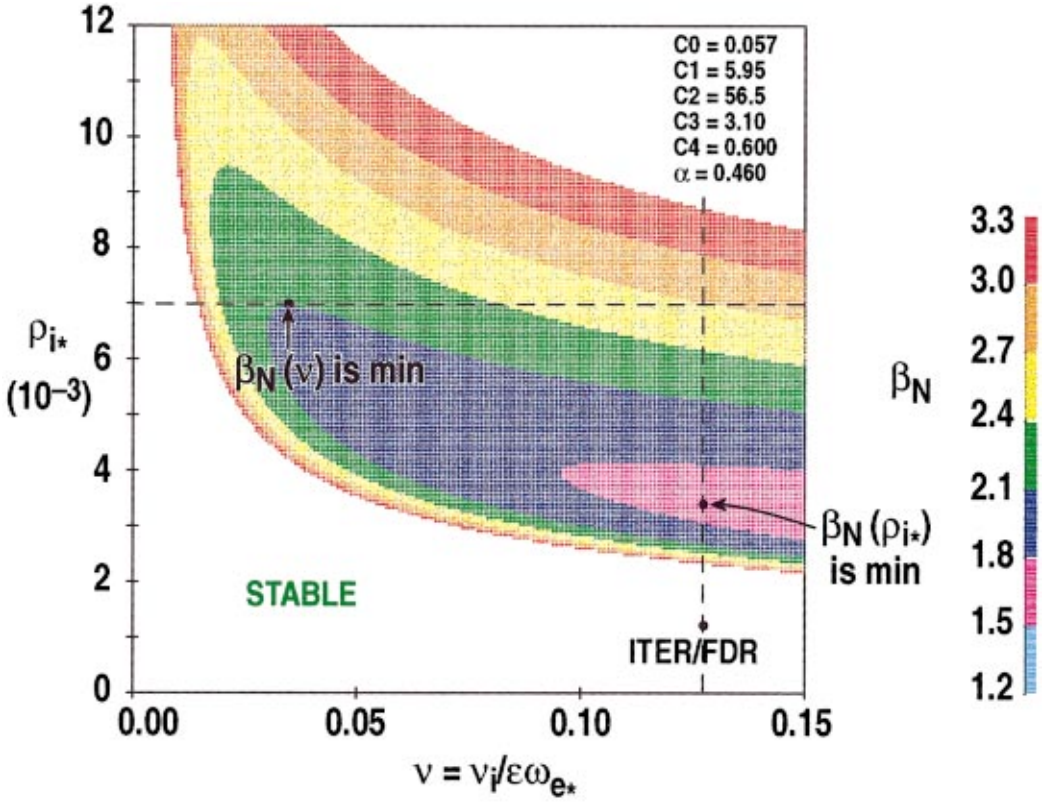

FIG. 8. (Color) Contour plots of critical β_N fit for $q=1$ sawtooth induced $m/n=3/2$ NTM in ρ_{i*}, ν space. Each β_N contour is 0.3 wide. Minima for $\rho_{i*}\equiv7.0\times10^{-3}$ with varying ν and for $\nu=0.13$ with varying ρ_{i*} are noted. The expected ITER/FDR operating point is in the stable region where the seed island is too small to excite the metastable tearing mode.

For ITER/FDR: (1) $w_{\rm pol}^2 \approx 0.5 w_d^2$ and the incomplete pressure flattening threshold is relatively larger, a consequence of the assumed $w_{\rm pol} \propto \rho_{i*}$ and $w_d \propto \rho_{i*}^{1/3}$ scalings, (2) the ratio of $w_{\rm seed}$ to $(w_{\rm pol}^2 + w_d^2)^{1/2}$ is about 0.6 or too small to excite the NTM, and (3) the first term in the denominator of the critical beta model Eq. (14) is approximately 0.38, which contributes to the threshold and stability, i.e., net negative denominator.

The best fit parameter $\alpha = 0.46 \pm 0.08$, to one sigma uncertainty, and characterizes the effect of dynamic coupling of the $q=1$ sawtooth instability as a source of $m/n=3/2$ seed island. $\alpha = 0.46 \pm 0.05$ from the seed island scaling shown in Fig. 5 which is *not* used in the beta fit and therefore provides an independent check on the consistency of the model. The consequence is that the ratio of $w_{\rm seed}$ to $w_{\rm pol}$ scales at fixed ν as $w_{\rm seed}/w_{\rm pol} \propto \rho_{i*}^{3\alpha-1} \propto \rho_{i*}^{0.38 \pm 0.24}$. Clearly, the uncertainty is high, and at the one-sigma confidence level, α could be too low (i.e., a weak scaling of $w_{\rm seed}/w_{\rm pol}$) to avoid seed islands exceeding the threshold island width, so NTMs would then *not* be avoided in ITER/FDR at low ρ_{i*}. This indicates the importance of an accurate determination of α. Including the incomplete pressure flattening threshold does still allow a reduced stable operating window of ITER/FDR but the w_d/r scaling is much more uncertain, both theoretically and from fitting to existing devices (as $w_d \ll w_{\rm pol}$) than that of $w_{\rm pol}/r$.

The best fit contour plot of critical β_N versus ρ_{i*} and $\nu = \nu_i/\epsilon\omega_{e*}$ is shown in Fig. 8. Comparison with Fig. 7 shows: (1) a region of increasing critical β_N with increasing ρ_{i*} and increasing ν similar to Fig. 7(a) for ASDEX Upgrade and DIII-D, (2) a region of increasing critical β_N with increasing ρ_{i*} and decreasing ν similar to Fig. 7(b) for JET, (3) minima in $\beta_N(\nu)$ at fixed ρ_{i*} which shift higher in ν as ρ_{i*} is lowered, as given by Eq. (12), (4) minima in $\beta_N(\rho_{i*})$ at fixed ν in the low ρ_{i*}, high ν region which has not been plumbed by existing devices, and (5) a stable region in which the seed island is too small to overcome the polarization/inertial and incomplete pressure flattening thresholds. The predicted ITER/FDR operating point ($\beta_N = 2.5$, $G = 1.35$, $\rho_{i*} = 1.2 \times 10^{-3}$, and $\nu = \nu_i/\epsilon\omega_{e*} = 0.13$) sits in the stable region. However, statistical uncertainty in fitting α and the reliance on both the seed and threshold islands becoming small at low ρ_i/high S reduces confidence in NTM avoidance in ITER/FDR, and it would thus be wise to continue the development of mode control techniques.

V. CONCLUSIONS

A database was assembled in terms of the critical beta for onset of a $q=1$ sawtooth induced $m/n=3/2$ neoclassical tearing mode. The operating regimes of the tokamaks ASDEX Upgrade, DIII-D, and JET were run as close as possible in shape, q_{95}, etc. to that proposed for the reactor-grade tokamak design ITER/FDR. The database is couched in terms of normalized beta, β_N, normalized size, ρ_{i*}, and normalized ion collisionality, $\nu = \nu_i/\epsilon\omega_{e*}$.

The database is fitted to a model based on physics first principles, not a purely empirical scaling law. The key physics points used are: (1) the dominant threshold island for NTMs is suggested from the polarization/inertial model of Wilson *et al.*, and (2) the seed island scaling is suggested from a model of Hegna *et al.* which takes into account the dynamical effect of geometrically coupled perturbation of the sawtooth instability, at the $q=3/2$ surface. The polarization/inertial threshold is successful in readily giving a nearly linear scaling of critical β_N with ρ_{i*} for the existing devices. The dynamic coupling effect on the seed island scaling is successful in explaining the change in the sign of the power of the v scaling from ASDEX Upgrade and DIII-D to JET, i.e., at smaller ρ_{i*}, higher magnetic Reynolds number S.

The best fit of the model was made using as few free parameters as possible, with no allowance for variations in profile factors such as the classical tearing stability parameter Δ', and thus can only be considered as representative of the existing devices. The common regime of $q(0) \approx 1$ due to sawteeth and similar q_{95} in ELMing H-mode should make for similar q and current profiles and thus similar values of Δ'. A key feature of the physics model and fit is a relative scaling of the ratio of seed island to polarization/inertial threshold island of $w_{\rm seed}/w_{\rm pol} \propto \rho_{i*}^{0.38 \pm 0.24}$, at fixed collisionality. This leads to a prediction for ITER/FDR, at very low ρ_{i*}, that the seed island could be too small to overcome the combination of the polarization/inertial and the incomplete pressure flattening thresholds due to dynamical decoupling of $q=1$ sawteeth to $q=3/2$ at high S. Thus the sawtooth would not sufficiently disturb the metastable plasma to trigger the NTM. However, the uncertainty in the fit to the existing database is such that additional data, particularly at lower ρ_{i*}, are needed to improve confidence in the extrapolation, and the continued development of control techniques is advisable.

Use of this particular $m/n=3/2$ NTM fit for other modes such as the ''hard'' $m/n=2/1$ NTM or to other regimes (different shape, q_{95}, etc.) is not recommended. Future work should continue to expand the database and fits to other cases (for example, for the $m/n=2/1$ mode or for advanced tokamaks with minimum $q>2$ and $m/n=5/2$ NTMs). Theoretical effort should concentrate on improving our understanding of the basic physics, particularly in the area of the threshold physics and trigger mechanisms (e.g., seed islands). The work presented here suggests that our theoretical model can describe several factors observed in the database. Nevertheless, the theory behind the model needs to be put on a firmer basis in order to develop a better predictive capability.

ACKNOWLEDGMENTS

We would like to thank the ASDEX Upgrade, DIII-D, and JET teams for the operations and diagnostics which made this collaboration possible. One of us (R.J.L.) thanks James Leuer for the ITER/FDR cross-section plot.

This work was supported by the U.S. Department of Energy under Contract No. DE-AC03-99ER54463, the United Kingdom Department of Trade and Industry, and EURATOM.

[1] P. H. Rutherford, Phys. Fluids **16**, 1903 (1973).
[2] Z. Chang, J. D. Callen, E. D. Fredrickson, R. V. Budny, C. C. Hegna, K. M. McGuire, and M. C. Zarnstorff, Phys. Rev. Lett. **74**, 4663 (1995).
[3] S. Günter, A. Gude, M. Maraschek, and Q. Yu, Plasma Phys. Controlled Fusion **41**, 767 (1999).

[4]R. J. La Haye and O. Sauter, Nucl. Fusion **38**, 987 (1998).
[5]G. T. A. Huysmans, *Proceedings of the 17th International Atomic Energy Agency Fusion Energy Conference*, Yokohama, 1998 (International Atomic Energy Agency, Vienna, 1999), IAEA-F1-CN-69/EXP3103.
[6]F. W. Perkins, D. E. Post, N. A. Uckan *et al.*, Nucl. Fusion **39**, 2137 (1999).
[7]O. Sauter, R. J. La Haye, Z. Chang *et al.*, Phys. Plasmas **4**, 1654 (1997).
[8]R. Fitzpatrick, Phys. Plasmas **2**, 825 (1995).
[9]S. Günter, A. Gude, M. Maraschek, S. Sesnic, and H. Zohm, Nucl. Fusion **38**, 1431 (1998).
[10]H. R. Wilson, J. W. Connor, R. J. Hastie, and C. C. Hegna, Phys. Plasmas **3**, 248 (1996).
[11]C. C. Hegna, J. D. Callen, and J. R. La Haye, Phys. Plasmas **6**, 130 (1999).
[12]M. N. Rosenbluth, private communication, 1999.
[13]R. Fitzpatrick, Nucl. Fusion **33**, 1045 (1993).
[14]D. Gates, B. Lloyd, A. W. Morris, G. McArdle, M. O'Brien, M. Valovic, C. N. Warrick, and H. R. Wilson, Nucl. Fusion **37**, 1593 (1997).
[15]S. M. Wolfe, R. S. Granetz, A. E. Hubbard, I. H. Hutchinson, J. H. Irby, and J. Ramos, Bull. Am. Phys. Soc. **43**, 1918 (1998).
[16]Y. Kamada, A. Isayama, T. Oikawa *et al.*, Nucl. Fusion **39**, 1845 (1999).
[17]A. Isayama, Y. Kamada, T. Ozeki, and N. Isei, Plasma Phys. Controlled Fusion **41**, 35 (1999).
[18]A. Gude, S. Günter, and S. Sesnic, Nucl. Fusion **39**, 127 (1999).
[19]R. J. La Haye, B. W. Rice, and E. J. Strait, Nucl. Fusion **40**, 53 (2000)
[20]Z. Chang and J. D. Callen, Nucl. Fusion **34**, 1309 (1994).
[21]R. J. La Haye, L. L. Lao, E. J. Strait, and T. S. Taylor, Nucl. Fusion **37**, 397 (1999).
[22]M. Maraschek, S. Günter, and H. Zohm, Plasma Phys. Controlled Fusion **41**, L1 (1999).
[23]Z. Chang, E. D. Fredrickson, S. H. Batha, M. G. Bell, R. V. Budny, F. M. Levinton, K. M. McGuire, G. Taylor, and M. Z. Zarnstorff, Phys. Plasmas **5**, 1076 (1998).
[24]C. Ren, M. S. Chu, and J. D. Callen, Phys. Plasmas **6**, 1203 (1999).
[25]J. P. Meskat, *Proceedings of the 26th European Physical Society Conference on Controlled Fusion and Plasma Physics*, Maastricht, 1999 (European Physical Society, Petit-Lancy, 1999), Vol. 23J, p. 1377.
[26]C. M. Bishop, J. W. Connor, R. J. Hastie, and S. C. Cowley, Plasma Phys. Controlled Fusion **33**, 398 (1991).